AIP Advances

Precision locking CW laser to ultrastable optical frequency comb by feed-forward method

Cite as: AIP Advances **9**, 115003 (2019); https://doi.org/10.1063/1.5121860
Submitted: 30 July 2019 . Accepted: 27 October 2019 . Published Online: 12 November 2019

X. D. Shao, H. N. Han, Y. B. Su, H. B. Wang, Z. Y. Zhang, S. B. Fang, G. Q. Chang, and Z. Y. Wei

Precision locking CW laser to ultrastable optical frequency comb by feed-forward method

Cite as: AIP Advances 9, 115003 (2019); doi: 10.1063/1.5121860
Submitted: 30 July 2019 • Accepted: 27 October 2019 •
Published Online: 12 November 2019

View Online Export Citation CrossMark

X. D. Shao,[1,2] H. N. Han,[1,a)] Y. B. Su,[1,3] H. B. Wang,[1,3] Z. Y. Zhang,[1,2] S. B. Fang,[1] G. Q. Chang,[1] and Z. Y. Wei[1,2,4,b)]

AFFILIATIONS

[1] Beijing National Laboratory for Condensed Matter Physics, Institute of Physics, Chinese Academy of Sciences, Beijing 100190, China
[2] University of Chinese Academy of Science, Beijing 10049, China
[3] School of Physics and Optoelectronics Engineering, Xidian University, Xi'an 710071, China
[4] Songshan Lake Materials Laboratory, Dongguan, Guangdong 523808, China

[a)] **Author to whom correspondence should be addressed:** hnhan@iphy.ac.cn
[b)] **E-mail:** zywei@iphy.ac.cn

ABSTRACT

We locked a 1064 nm continuous wave (CW) laser to a Yb:fiber optical frequency comb stabilized to an ultrastable 972 nm CW laser with the feed-forward method. Consequently, the stability and coherent properties of the ultrastable laser are precisely transferred to the 1064 nm CW laser through the frequency comb's connection. The relative linewidth of the frequency-stabilized 1064 nm CW laser is narrowed to 1.14 mHz, and the stability reaches 1.5×10^{-17}/s at the optical wavelength of 1064 nm. The phase noise characterization in the 1 mHz–10 MHz range is presented to indicate that feed-forward locking a CW laser to an ultrastable comb will offer a potential technique for many important applications, such as optical frequency synthesis and gravitational wave detection.

Optical frequency comb (OFC) and frequency-stabilized continuous wave (CW) lasers are two key components in many applications such as optical clocks, high-resolution spectroscopy, time and frequency transfer, astrocombs, absolute distance measurement, coherent property transfers in optical fields, and space-based gravitational wave detection.[1–8] In all the above applications, coherent locking between an OFC and a CW laser is generally required. A traditional connection technique is based on a servo phase-locked loop (PLL) electronics that generates appropriate control signals, which are fed back to control the actuators (e.g., the piezoelectric transducer, the acoustic optical modulator, the pump current, or the temperature of the system) in laser. Locking an OFC to a CW laser or locking a CW laser to an OFC has been accomplished with the servo feedback phase-locked loop method in the past few decades.[9–13] However, the PLL electronics with large servo bandwidth requires more complex circuit design and more careful adjustment of P-I filter parameters. Although a wide bandwidth locking up to 1.3 MHz in the extended cavity diode laser (ECDL) has been obtained by direct feedback control of the injection current of the diode laser with error signal,[14] in most solid-state lasers and fiber lasers, the locking bandwidth of the whole system is usually limited to less than 200 kHz by the properties of the actuator, the noise introduced by a complex circuit, and the pump-gain process. Taking an example of the impact of the solid-state gain medium, in the Ti:sapphire comb, the upper level lifetime of the Ti:sapphire medium is 3.2 μs, which corresponds to the theoretical servo bandwidth of 300 kHz, but in the case of locking the carrier-envelope phase offset (CEO) frequency with the PLL electronics, it typically only reaches approximately 50 kHz.[15]

In 2011, a novel feed-forward method, based on an acousto-optic frequency shifter (AOFS) without the PLL, was developed to stabilize the carrier envelope phase offset (CEO) signal in OFCs.[16] Due to the real time response for frequency shift in the AOFS, the CEO control decreased dramatically to 12 as the residual timing jitter was successfully obtained in the Ti:sapphire comb. Since then, the feed-forward configuration has been used in multiple OFCs, such as fiber comb, to minimize the CEO phase noise.[17,18] In 2012, this scheme was adopted in locking the CW laser to the frequency comb by Sala *et al.*[19,20] The ~0.6 MHz feed-forward locking bandwidth and the ~10 kHz linewidth in the locked CW laser have been demonstrated.

In this letter, we demonstrated an ultranarrow linewidth 1064 nm CW laser by applying the feed-forward method to lock to a Yb:fiber OFC that was stabilized to an ultrastable 972 nm CW laser.[21] The 1064 nm laser beam was separated into a transmitted beam and a first-order diffracted beam with the AOFS. To lock and analyze the 1064 nm CW laser, the beat signals between the comb and these two beams were recorded by in-loop and out-of-loop configurations. The relative linewidth of the out-of-loop beat note was reduced to 1.14 mHz after feed-forward locking the 1064 nm laser to the comb, which was the first time the megahertz-level was accessed by the feed-forward locking technique. Over 3 h of measuring, the frequency shift showed an Allan deviation of 1.5×10^{-17} in a 1 s sampling rate. We also measured the phase noise power spectral density (PSD) of the stabilized out-of-loop beat note signal from 1 mHz to 10 MHz. The integrated phase noise (IPN) was 381 mrad from 1 Hz to 10 MHz, which corresponds to 216 as timing jitter in a 1 s series. Accordingly, the IPN from 1 mHz to 10 Hz was 20.5 mrad, which corresponds to 11.5 as timing jitter in a long 1000 s series. This long-term frequency stability and extremely low phase noise, especially in a low frequency regime, are of particular importance for the applications of optical frequency synthesis and gravitational wave detection.

The experimental setup is shown in Fig. 1. The 1064 nm CW laser is a diode-pumped monolithic Nd:YAG laser that operates at single frequency with 500 mW output power.[22] The laser is prestabilized to one of the absorption spectral lines of iodine molecules ($^{127}I_2$).[23,24] Due to not strictly controlling the temperature of the iodine molecule chamber and eliminating the residual amplitude modulation, the frequency offset of the 1064 nm CW laser still has a few kilohertz jitter in short term and dozens of kilohertz drift in long term after prestabilization.[25] This prestabilized 1064 nm CW laser benefits to the further locking to the ultrastable comb; however, since the 1064 nm CW laser has previously been locked into the absorption spectral lines of iodine molecules, it is difficult to be further locked to an ultrastable comb by feedback internal or external ports to modulate the laser cavity. For this setup, the feed-forward method, just to change the output laser beam frequency instead of modulating any laser cavity internal parameters, is a good solution. The optical frequency comb is based on a 250 MHz, 20 mW, 1030 nm Yb-doped fiber comb that has been stabilized to an ultrastable 972 nm CW tunable diode laser, which has been locked to a high fineness F-P cavity with the Pound-Drever-Hall (PDH) technique. The relative stability of the Yb:fiber comb was reported to reach 2 × 10–18/s, one of the best in Yb:fiber combs, as described in Ref. 21.

To complete the feed-forward locking between the 1064 nm laser and the ultrastable comb, an AOFS at a center modulation frequency of 80 MHz was inserted into the beam from the 1064 nm CW laser. Its modulation bandwidth is approximately 1.4 MHz, which provides an availability of wide bandwidth phase locking. When the deflection efficiency of the AOFS was set to 10%, the 1064 nm laser beam was divided into a transmitted beam with 450 mW (in-loop) and a first-order diffracted beam with 50 mW (out-of-loop). They were then separately superimposed and heterodyned with the nearest line of the Yb:fiber comb.

A self-heterodyne fiber delay technique was used to evaluate the spectral content of both the first order diffracted beam and the frequency comb in Refs. 19 and 20. In our experiment, as the ultrastable laser that the Yb:fiber comb has been locked to has a narrow linewidth on the hertz-level, which means very long coherence length, the self-heterodyne fiber delay technique is not appropriate here. Hence, we build the out-of-loop to detect the beat signal between the first-order diffracted beam and the comb to assess the phase noise characterization of the stabilized CW 1064 nm laser. In the in-loop interferometer, the beat signal was detected by using a photodiode (PD), $f_{in\text{-}loop} = |f_n - f_{cw}|$, where f_n is the nth comb mode

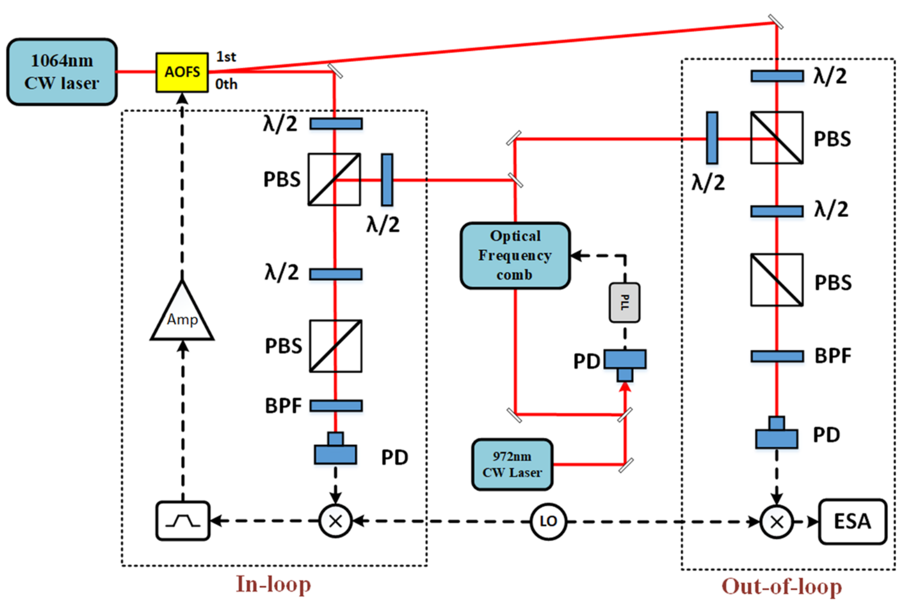

FIG. 1. Experimental setup. AOFS: acoustic-optical frequency shifter, PBS: polarizing beam splitter, λ/2: half-wavelength plate, Amp: RF signal amplification, LO: RF synthesizer, BPF: bandpass filter, PLL: phase locked loop, PD: photodiode, and ESA: electrical spectrum analyzer. Red solid line: optical path, and black dashed line: electronic loop.

and f_{cw} is the CW laser frequency. The $f_{in\text{-}loop}$ was then mixed with an RF synthesizer (LO) signal, f_{LO}, which is derived from the frequency synthesizer to generate the driving signal of the AOFS, f_{AOFS}. Thus, it has been shown that $f_{AOFS} = f_{LO} \mp f_{in\text{-}loop}$. In the out-of-loop interferometer, the beat frequency, $f_{out\text{-}of\text{-}loop}$, heterodyned between the first-order diffracted beam and the comb, which can be expressed as

$$\begin{aligned} f_{out\text{-}of\text{-}loop} &= f_n - \left(f_{cw} + f_{AOFS}\right) \\ &= f_n - \left[\left(f_n \pm f_{in\text{-}loop}\right) + \left(f_{LO} \mp f_{in\text{-}loop}\right)\right] \\ &= f_{LO}. \end{aligned} \tag{1}$$

From this equation, it is clear that the $f_{out\text{-}of\text{-}loop}$ is stabilized at the frequency f_{LO}, and the noise carried by f_{cw} is removed by the $f_{in\text{-}loop}$ with the opposite signs in terms of f_{cw} and f_{AOFS}.

In one experiment, we obtained the beat signal of about 22.2 MHz and mixed it with an RF signal of 102.2 MHz to obtain the 80 MHz driving signal for the AOFS. According to Eq. (1), the $f_{out\text{-}of\text{-}loop}$ should be fixed at 102.2 MHz after being locked. Figure 2 shows the $f_{out\text{-}of\text{-}loop}$ beat note frequency spectrum and the linewidth after locking. The frequency spectrum content of $f_{out\text{-}of\text{-}loop}$ is recorded by using the frequency spectrum analyzer (R&S, FSW26) with 1 kHz resolution bandwidth. The $f_{out\text{-}of\text{-}loop}$ had a 45 dB signal-to-noise ratio and contained more than 90% of RF power within the coherent carrier. In addition, two bumps appear at approximately 0.28 MHz on both sides of the center frequency, $f_{out\text{-}of\text{-}loop}$, indicating that the actual bandwidth of the whole feed-forward system is approximately 280 kHz. This was dependent on the rising time of acoustic wave transmission in the AOFS. To investigate the exact relative linewidth of $f_{out\text{-}of\text{-}loop}$, we used a fast Fourier transform (FFT) analyzer (SRS, SR770) with the resolution bandwidth of 0.47 mHz to measure the frequency spectrum distribution. The curve in Fig. 2(b) shows that the original data points match a Lorentzian line shape, and the relative linewidth is reduced to 1.14 mHz.

We also compared the frequency shift of the $f_{out\text{-}of\text{-}loop}$ in a long time series by a frequency counter using the 1064 nm CW laser with and without feed-forward locking to the comb. When the 1064 nm CW laser was in the condition of pre-iodine-stabilization, the $f_{out\text{-}of\text{-}loop}$ had a kilohertz of jitter in a 1 s time gate and dozens of kilohertz of drift in the long term, dropping from 40 kHz to −40 kHz over a 1.8 h time period, shown by the blue shade in Fig. 3(a). After feed-forward locking to the ultrastable comb, both the fast jitter and the slow shift in the $f_{out\text{-}of\text{-}loop}$ were depressed to a large extent. The red line in Fig. 3(a) represents the frequency drift of the stabilized $f_{out\text{-}of\text{-}loop}$, like a straight line without any fluctuation compared to the blue curve. The detail over the 3-h time period of the stabilized $f_{out\text{-}of\text{-}loop}$ is described in Fig. 3(b), which corresponds to a 4.1 mHz standard deviation of the shift. The calculated Allan deviation is shown in Fig. 3(c) with a tracking stability of 1.5×10^{-17} in a 1 s sampling rate at the central wavelength of 1064 nm, where the tracking stability dropped below 2.7×10^{-19} at 1000 s gate time. This was attributed to the AOFS with ~1.4 MHz frequency mismatch tolerance, which was larger than in the general servo-loop circuit.

For a deeper look at the noise performance, the phase noise power spectral density (PSD) and the integrated phase noise (IPN) of the locked $f_{out\text{-}of\text{-}loop}$ were observed in frequency-resolved 1000 s (1 mHz–10 MHz). We could not measure the PSD of the free running beat note signal $f_{out\text{-}of\text{-}loop}$ because of strong jitter in the regime of exceeding 1 s where the analyzer was unable to read the data. At high frequencies, from 1 Hz to 1 MHz, as shown in Fig. 4(a), the total IPN was 381 mrad, which corresponded to 216 as timing jitter. The inflection point at 280 kHz across the PSD distribution reflected the bandwidth of the feed-forward scheme, in accordance with the analysis of Fig. 2(a). The 80% of residual integrated phase noise originated from outside the servo bandwidth, and the noise below hundreds of kilohertz was well suppressed. Figure 4(b) shows the low frequency noise, characterized from 1 mHz to 10 Hz, measured with the FFT analyzer. The IPN from 1 mHz to 10 Hz was 20.5 mrad, which corresponded to 11.6 as residual timing jitter. When transformed to the frequency noise amplitude spectral density in the unit of Hz/$\sqrt{\text{Hz}}$, the noise amplitude was 2×10^{-3} Hz/$\sqrt{\text{Hz}}$ in 1 mHz. It is worth noting that a CW laser with such low IPN

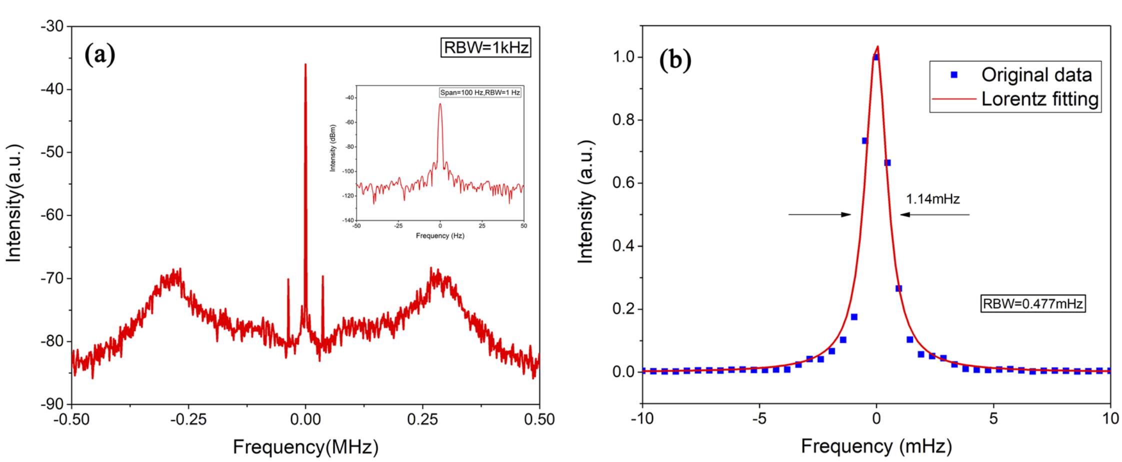

FIG. 2. The frequency spectrum and relative linewidth of beat note signals after locking. (a) Frequency spectrum of the beat note signal $f_{out\text{-}of\text{-}loop}$ at RBW = 1 kHz. The inset at RBW = 1 Hz. (b) The relative linewidth of $f_{out\text{-}of\text{-}loop}$ is recorded with the blue point (RBW = 0.47 mHz). Under Lorentz fitting (red line), the linewidth is 1.14 mHz.

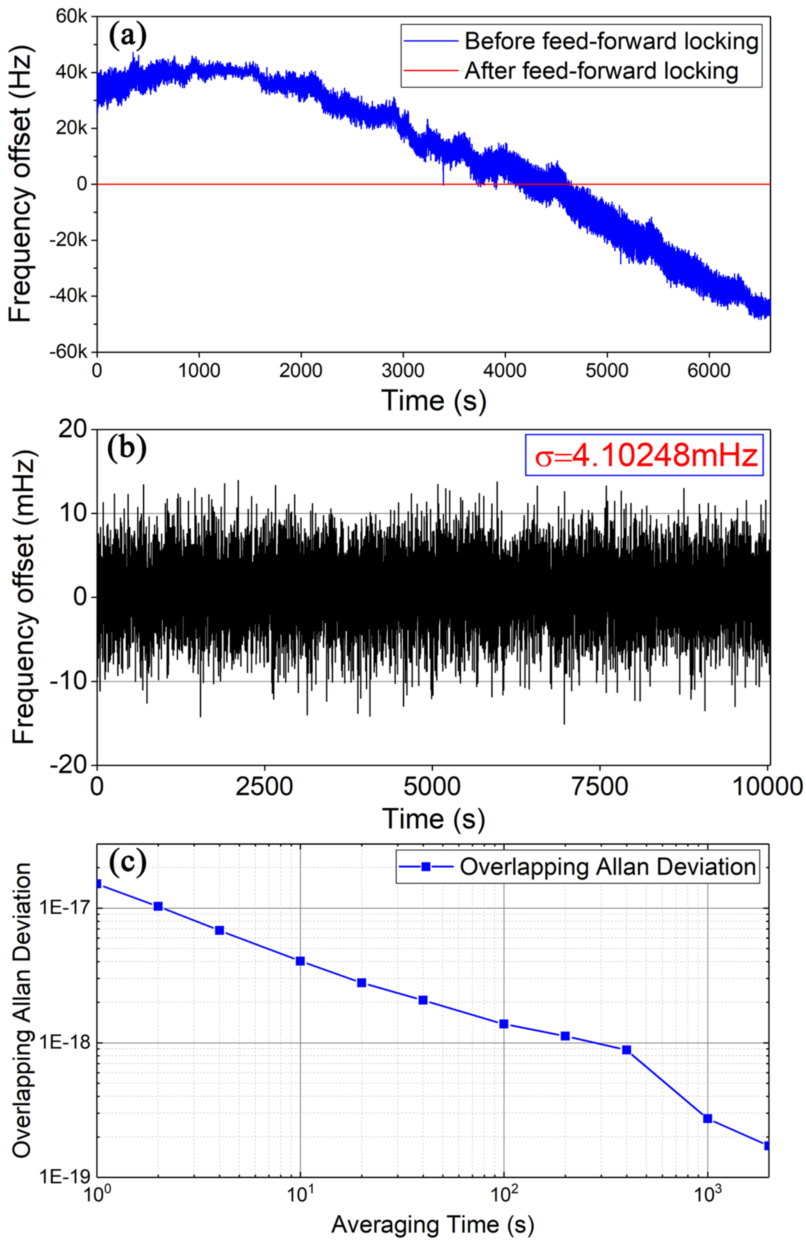

FIG. 3. The frequency stability of the 1064 nm CW laser in time domain. (a) The comparison of the frequency offset of the 1064 nm CW laser before and after feed-forward locking. (b) The frequency offset for approximately 3 h recorded by the counter at 1 s gate time with feed-forward locking. (c) The corresponding Allan deviation to the optical frequency ν_{opt} (λ_{opt} = 1064 nm).

in the low frequency range benefits the detection of low frequency gravitational waves.[26]

In conclusion, we demonstrated that precision locking can occur between a 1064 nm CW laser and an ultrastable optical frequency comb by the feed-forward method without the servo-loop. The out-of-loop measurements confirmed that the stability and coherent properties of the ultrastable comb were transferred to the 1064 nm CW laser. The relative linewidth of the stabilized CW 1064 nm laser was narrowed to 1.14 mHz, and the Allan deviation was 1.5×10^{-17} in 1 s, which is on the same scale of the ultrastable comb. The integrated phase noises in the range of the high frequencies (1 Hz–10 MHz) and low frequencies (1 mHz–10 Hz) reached 381 mrad and 20.5 mrad, respectively. The long-term stability and the phase noise have shown the robustness and reliability of the feed-forward scheme and indicate that such a stabilized CW laser may find important applications in low frequency gravitational wave detection and high precision optical frequency synthesis. In the future, we will lock multiwavelength CW lasers to ultrastable frequency comb with the feed-forward scheme to establish an ultrastable and ultraprecise optical frequency synthesizer.

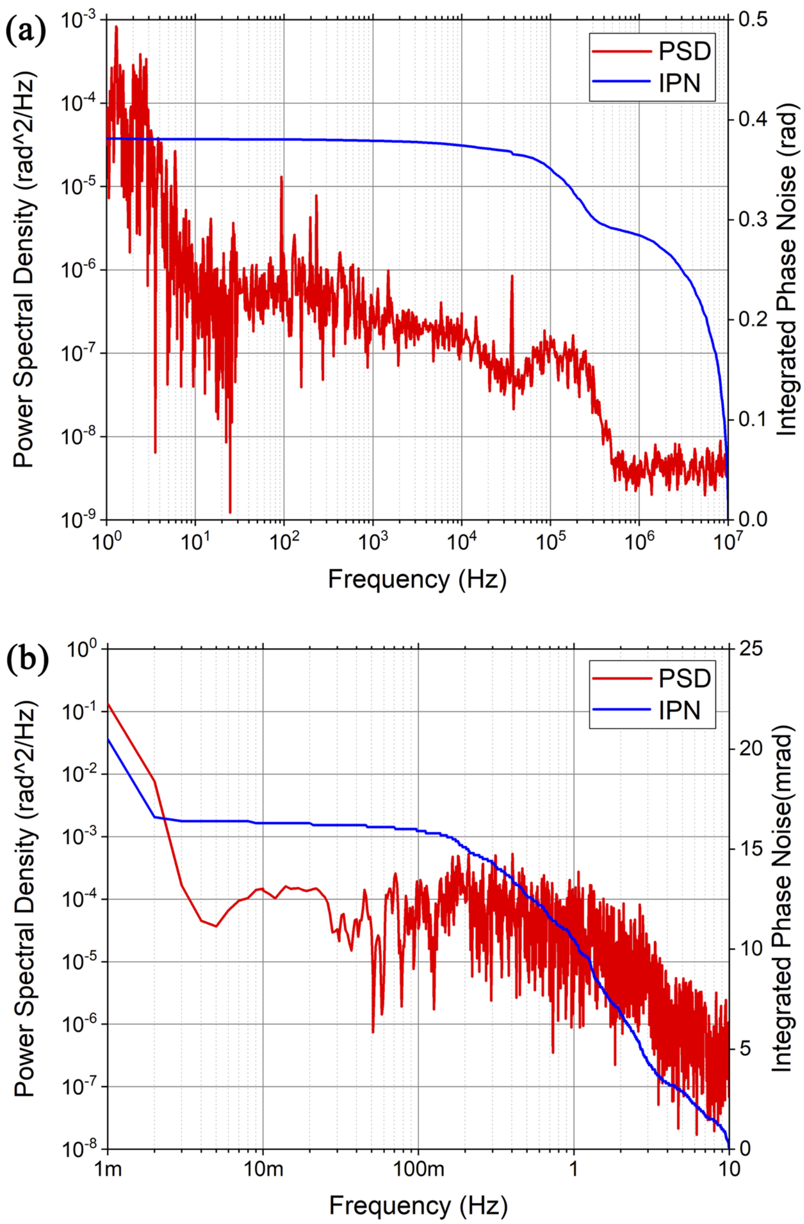

FIG. 4. The noise characteristic of the $f_{out\text{-}of\text{-}loop}$ beat note. (a) The power spectral density (red) and integrated phase noise (blue) from 1 Hz to 10 MHz. (b) The low frequency power spectral density (red) and integrated phase noise (blue) from 1 mHz to 10 Hz.

This work was funded by the Strategic Priority Research Program of the Chinese Academy of Sciences (Grant Nos. XDA1502040404, XDB21010400, and XDB23030230) and the National Natural Science Foundation of China (NSFC) (Grant Nos. 61575219, 11774234, 91850209, and 11434016).

REFERENCES

[1] F. R. Giorgetta, W. C. Swann, L. C. Sinclair, E. Baumann, I. Coddington, and N. R. Newbury, Nat. Photonics **7**, 434–438 (2013).

[2] R. A. McCracken, J. M. Charsley, and D. T. Reid, Opt. Express **25**, 15058–15078 (2017).

[3] D. Nicolodi, B. Argence, W. Zhang, R. Le Targat, G. Santarelli, and Y. Le Coq, Nat. Photonics **8**, 219–223 (2014).

[4] T. Rosenband, D. B. Hume, P. O. Schmidt, C. W. Chou, A. Brusch, L. Lorini, W. H. Oskay, R. E. Drullinger, T. M. Fortier, J. E. Stalnaker, S. A. Diddams, W. C. Swann, N. R. Newbury, W. M. Itano, D. J. Wineland, and J. C. Bergquist, Science **319**, 1808–1812 (2008).

[5] M. Tinto and N. Yu, Phys. Rev. D **92**, 042002 (2015).

[6] T. Udem, R. Holzwarth, and T. W. Hansch, Nature **416**, 233–237 (2002).

[7] S. Hyun, Y. J. Kim, Y. Kim, and S. W. Kim, CIRP Ann. **59**, 555–558 (2010).

[8] X. L. Shen, M. Yan, Q. Hao, K. W. Yang, and H. P. Zeng, IEEE Photonics J. **10**, 1 (2018).

[9] C. P. McRaven, M. J. Cich, G. V. Lopez, T. J. Sears, D. Hurtmans, and A. W. Mantz, J. Mol. Spectrosc. **266**, 43–51 (2011).

[10]L. S. Ma, Z. Y. Bi, A. Bartels, L. Robertsson, M. Zucco, R. S. Windeler, G. Wilpers, C. Oates, L. Hollberg, and S. A. Diddams, Science **303**, 1843–1845 (2004).
[11]J. Jin, Y. J. Kim, Y. Kim, and S. W. Kim, Opt. Express **14**, 5968–5974 (2006).
[12]T. R. Schibli, K. Minoshima, F. L. Hong, H. Inaba, Y. Bitou, A. Onae, and H. Matsumoto, Opt. Lett. **30**, 2323–2325 (2005).
[13]E. Benkler, F. Rohde, and H. R. Telle, Opt. Lett. **38**, 555–557 (2013).
[14]D. Akamatsu, Y. Nakajima, H. Inaba, K. Hosaka, M. Yasuda, A. Onae, and F. L. Hong, Opt. Express **20**, 16010–16016 (2012).
[15]K. W. Holman, R. J. Jones, A. Marian, S. T. Cundiff, and J. Ye, IEEE J. Sel. Top. Quantum Electron. **9**, 1018–1024 (2003).
[16]S. Koke, C. Grebing, H. Frei, A. Anderson, A. Assion, and G. Steinmeyer, Nat. Photonics **4**, 462–465 (2010).
[17]M. Yan, W. X. Li, K. W. Yang, H. Zhou, X. L. Shen, Q. Zhou, Q. T. Ru, D. B. Bai, and H. P. Zeng, Opt. Lett. **37**, 1511–1513 (2012).
[18]B. J. Fong, W. T. Lin, S. Y. Wu, J. L. Peng, W. W. Hsiang, and Y. Lai, Opt. Lett. **40**, 966–969 (2015).
[19]T. Sala, D. Gatti, A. Gambetta, N. Coluccelli, G. Galzerano, P. Laporta, and M. Marangoni, Opt. Lett. **37**, 2592–2594 (2012).
[20]D. Gatti, T. Sala, A. Gambetta, N. Coluccelli, G. N. Conti, G. Galzerano, P. Laporta, and M. Marangoni, Opt. Express **20**, 24880–24885 (2012).
[21]L. H. Pang, H. N. Han, Z. B. Zhao, W. J. Liu, and Z. Y. Wei, Opt. Express **24**, 28993–29000 (2016).
[22]Z. Erjun, C. A. O. Jianping, L. I. Ye, D. Yongkai, Y. Tao, L. I. Chengyang, and L. I. Wenbo, Chin. J. Lasers **34**, 203–208 (2007).
[23]J. L. Hall, L. S. Ma, M. Taubman, B. Tiemann, F. L. Hong, O. Pfister, and J. Ye, IEEE Trans. Instrum. Meas. **48**, 583–586 (1999).
[24]A. Arie and R. L. Byer, J. Opt. Soc. Am. B **10**, 1990–1997 (1993).
[25]E. A. Whittaker, M. Gehrtz, and G. C. Bjorklund, J. Opt. Soc. Am. B **2**, 1320–1326 (1985).
[26]O. Jennrich, Class. Quantum Gravity **26**, 153001 (2009).